Performance optimization for hard x-ray/soft gamma-ray detectors

Fiona A. Harrison, Steven M. Kahn, Charles J. Hailey, Klaus Ziock

Fiona A. Harrison, Steven M. Kahn, Charles J. Hailey, Klaus Ziock, "Performance optimization for hard x-ray/soft gamma-ray detectors," Proc. SPIE 1344, EUV, X-Ray, and Gamma-Ray Instrumentation for Astronomy, (1 November 1990); doi: 10.1117/12.23288

Event: 34th Annual International Technical Symposium on Optical and Optoelectronic Applied Science and Engineering, 1990, San Diego, CA, United States

Performance optimization for hard X-ray / soft γ-ray detectors

Fiona A. Harrison and Steven M. Kahn

University of California at Berkeley
Department of Physics and Space Sciences Laboratory
Berkeley, California 94720

Charles J. Hailey and Klaus P. Ziock

Lawrence Livermore National Laboratory
Livermore, California 94550

ABSTRACT

This paper discusses the optimization of the performance of imaging scintillation detectors used in the hard X-ray / soft γ -ray (20 - 300) keV region of the spectrum. In these devices, absorption of an incident γ -ray within an alkali halide crystal induces a scintillation light distribution which is centroided by an imaging photomultiplier tube mounted to the crystal. The ultimate imaging resolution is strongly affected by the detailed propagation of the scintillation light within the crystal and at the interface between the crystal and the phototube face plate. We have investigated a number of refined techniques for preparing the scintillation crystals so as to optimize the imaging resolution. Our results indicate very good agreement with relatively simple models of the light propagation. We show that it is possible to achieve resolution consistent with the most optimistic models.

1. INTRODUCTION

Imaging scintillation detectors have found wide application in recent years for hard X-ray / soft γ -ray imaging in fields ranging from medical physics to astronomy. In these detectors a γ -ray incident on an alkali halide crystal is converted to scintillation light. An imaging photomultiplier tube coupled to the scintillating crystal centroids the light distribution, measuring the interaction position of the incident γ -ray. Our particular application employs a commercial 3" square envelope Hamamatsu imaging phototube. Electrons ejected from the bialkali photocathode of this tube are amplified by a factor of about 2×10^5 in the dynode chain (typical operating voltage 1000 Volts) and collected on a crossed-wire anode. The dynodes are flat meshes which maintain the spatial integrity of the electron cloud during the amplification process. The anode wires are resistively coupled, and two signals for each dimension are read out the end wires using charge-sensitive preamplifiers. After electronic shaping and digitization, a simple charge division algorithm is used to determine the centroid of the charge cloud.

Employed in a coded aperture imaging system, the imaging scintillation detectors can provide a high angular resolution telescope. In a coded aperture telescope, a source distribution casts a γ-ray shadow of a partially-opaque mask onto an image plane. Subsequent post-processing of the resulting shadow pattern yields an image of the source distribution. We have developed such an instrument, the Gamma-Ray Arcminute Telescope Imaging System (GRATIS), designed to have arcminute angular resolution in the 30 - 200 keV band [1,2]. This instrument will be flown from a balloon-borne, stabilized platform next year.

Improved detector spatial resolution affords several advantageous design options for a coded aperture system. In coded aperture telescopes, the angular resolution is determined by the mask to detector plane separation and by the mask pixel size. To improve the angular resolution either the focal length can be increased or the pixel size decreased. The latter may require improved detector spatial resolution since the detector resolution must be good enough to adequately sample the mask pattern. There are additional ways, however, in which reduced pixel size can be applied. The pixel size and the focal length can both be decreased, with the angular resolution remaining constant, increasing the field of view of the telescope. This option is particularly applicable for a telescope employing commertial detectors of fixed active area. In addition, for these imaging scintillation detectors the resolution depends on the scintillating crystal's thickness, being better for thinner crystals. Improving the resolution with a crystal of given thickness can allow thicker crystals to be used without degrading the imaging performance, resulting in better quantum efficiencies at higher gamma-ray energies.

2. MODELING THE IMAGING PERFORMANCE

We have constructed a relatively simple model for the spatial resolution of the scintillation detectors. For γ-ray energies below a few hundred keV, Compton scattering can be neglected, significantly simplifying the calculation. With this omission, the error in the derived γ-ray position, $(\Delta x)_\gamma$, can be written in the form:

$$(\Delta x)_\gamma^2 = (1+\phi)\frac{(\Delta x)_c^2}{\overline{n}} + \frac{(\Delta x)_p^2}{g\overline{n}} + (\Delta x)_e^2 + (\Delta x)_f^2 .$$

Here, ϕ is the ratio of spatially uniform to spatially peaked components of the scintillation light, $(\Delta x)_c$ is the absorption-weighted spread in the scintillation light cloud, $\overline{n}$ is the mean number of photoelectrons per incident γ-ray (proportional to the γ-ray energy), $(\Delta x)_p$ is the "partition noise" spread resulting from the partition of the charge cloud among the various anode wires, g is the IPT gain, $(\Delta x)_e$ is the uncertainty introduced in the charge division algorithm by electronic noise, and $(\Delta x)_f$ is the spread introduced by emission and reabsorption of a fluorescent photon following the initial γ-ray interaction.

For a design optimized in the energy range 30 - 200 keV, the dominant contribution comes from the first term which is associated with the geometric broadening of the scintillation light distribution as it propagates through the crystal and the glass faceplate of the phototube. The partition noise term which also makes a measurable contribution to the spatial resolution, has been directly measured for the Hamamatsu phototube using a small optical fiber whose output signal is fixed at a known equivalent number of detected photoelectrons. The electronic noise term depends on the signal processing scheme but can be shown to be negligible for the electronics chain we are using with the image tube.

The final term can play an important role since the fluorescent photon is usually not reabsorbed at the precise position of the original photointeraction. Emission of a fluorescent photon is quite common (~ 86% of the interactions) in alkali halide crystals at energies above the K-edge. The contribution of this effect is energy and geometry dependent through the probability of escape of the fluorescent photon. We have carried out Monte Carlo simulations of this effect and found it to be unimportant in the energy range 30 - 200 keV, unless the crystals used are thinner than ~ 1 mm.

Since the geometric spreading of the scintillation light, $(\Delta x)_c$ is the dominant contribution to the detector spatial resolution we have concentrated our efforts on minimizing this spread. We use a Monte Carlo code to predict the effect that changing the crystal geometry will have on the light distribution striking the photocathode. The code treats the distribution as consisting of a spatially concentrated and a spatially uniform component. The spatially concentrated component consists of light which has undergone one or fewer reflections from the crystal surfaces, multiple reflections being treated as contributing to a uniform diffuse component. The reflections are treated as either specular or diffuse, depending on the crystal surface preparation.

3. TECHNIQUES FOR IMPROVING THE IMAGING PERFORMANCE

3.1 Surface preparation

Figure 1. Cartoon illustrating reflection off the top and bottome crystal surfaces for the specular case. Reflection off the top surface forms a virtual image lying above the crystal surface.

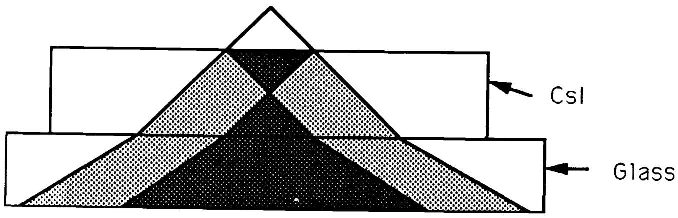

An important result is that for a fixed crystal thickness, the resolution depends dramatically on the crystal surface preparation. The best resolution is achieved for both top and bottom surfaces being diffuse reflectors. This is due to three effects. First, for rough surfaces, less light gets trapped within the critical angle by regular reflections. This trapped light eventually escapes, contributing to the uniform diffuse component, or is reabsorbed by the crystal. Secondly, as is illustrated in Figure 1, for a specular top surface, reflected light appears to be from a virtual image lying above the crystal surface and hence the light distribution at the photocathode is broader. Finally, since the index of refraction of the crystal is higher than that of glass, light striking the phototube faceplate always bends away from the surface normal. If the bottom surface is specular, this contributes more to the broadening of the light distribution.

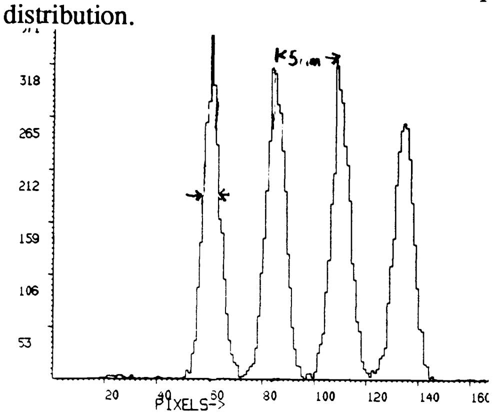

Figure 2b. Resolution at 60 keV for a 2 mm thick CsI(Na) crystal with specular surfaces.

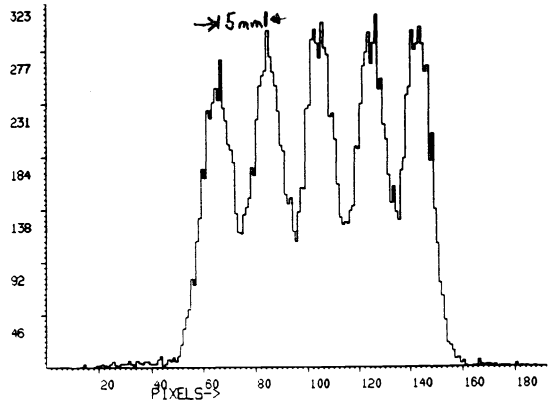

Figure 2a. Resolution at 60 keV for a 2 mm thick CsI(Na) crystal with rough surfaces.

Results from laboratory measurements show the magnitude of these effects. Figure 2a shows the resolution obtained using a series of pinhole images spaced 5 mm apart. The CsI(Na) crystal used to obtain this image is 2 mm thick and has both surfaces ground with coarse grit. Diffusely reflecting aluminum foil is loosely placed on the top crystal surface. The spatial resolution is 1.5 mm (FWHM) at 60 keV. Figure 2b shows pinhole images with the same 5 mm spacing taken with a 2 mm thick crytal which had both surfaces diamond turned to a specular finish (8 nm rms roughness) with specularly reflecting aluminum foil loosely placed on the top of the crystal. The resolution is 3.3 mm (FWHM).

Table 1 summarizes results of data taken using 2 mm thick crystals of various surface preparations. The scaling of the resolution with different surface preparations agrees well with our model.

Table 1: Results using a 2 mm crystal with various surfaces

top surface	bottom surface	FWHM resolution (mm) at 60 keV
specular	specular	3.3
specular	diffuse	2.5
diffuse	specular	2.0
diffuse	diffuse	1.5

We found that the most consistant, best results were obtained with crystals prepared with a coarse aluminum oxide grit and having approximately 3 micron rms surface roughness. Through experimenting with different preparation techniques we found that some finer grits tend to scratch the surfaces, resulting in uneven defects. Unprepared crystals from most vendors tend to have 500 - 1000 Angstrom rms roughness but with many coarse, regular surface defects. Grinding with coarse aluminum oxide yields a very even, regular surface.

3.2 Dependence on crystal thickness

For the crystals optimally prepared with diffuse surfaces we measured the dependence of the spatial resolution on the crystal thickness. The results are shown in Figure 3, and are consistant with predictions from the Monte Carlo model. The resolution scales roughly as the crystal thickness plus the glass phototube faceplate thickness. In our detectors, the glass faceplate is 3 mm thick, and so is the dominant contribution for thin crystals. For thick crystals the scaling is roughly linear in the crystal thickness. For crystals thicker than ~ 8 mm it appears that the light distribution is large enough that gain variations in the photocathode begin to contribute to the spatial resolution. This effect is also seen as a degradation in the energy resolution.

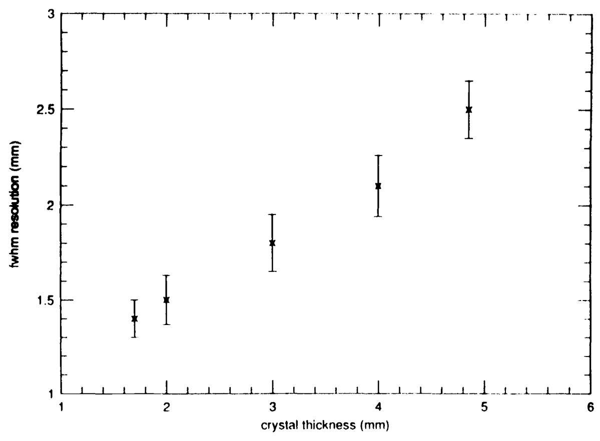

Figure 3. Experimental measurements of spatial resolution for crystals of different thicknesses measured at 60 keV.

3.3 Retroreflecting top crystal surface

A significant improvement in the spatial resolution can be achieved by making the top surface of the scintillating crystal a retro-reflector. This has the effect of redirecting the component of the scintillation light which is reflected off the top of the crystal, resulting in a narrower light distribution at the photocathode. Our Monte Carlo predicts that we should be able to achieve ~ 1 mm resolution for a 2.5 mm thick crystal. The retro-reflector we are developing is one-dimensional, consisting of a series of right-angle grooves with the improved resolution realized only in the dimension perpendicular to the grooves. For the detector's coded aperture application on GRATIS, improved spatial resolution is required in one dimension only[3].

The most effective way to produce the corner mirror pattern is to press a dye ruled with the pattern directly into the crystal surface. With this technique many crystals can be produced using the same dye, making the fabrication cost-effective. We also did not achieve optimal performance using a prefabracated corner reflector due to problems coupling it effectively to the crystal surface. The dye used to produce the groove pattern must have regular grooves with the correct profile, and the surfaces of the grooves must be specularly reflecting. We were able to produce an acceptable dye by ruled into a copper surface with a diamond ruling engine.

Pressing the dye into the crystal surface presents some practical problems. Applying enough pressure at room temperature to the crystal to impress the pattern causes severe fractures in the crystal beneath the surface. The crystal must be annealed in order to produce the pattern without causing plastic strains which reduce the scintillation efficiency. We have successfully pressed a test pattern into a crystal surface using this method, without reducing the scintillation efficiency. With this technique we expect to be able to produce grooved crystals in the near future which should allow us to achieve the expected improvement in the detector imaging performance.

4. CONCLUSION

Figure 4. Extrapolated resolution for a detector optimized for a given energy.

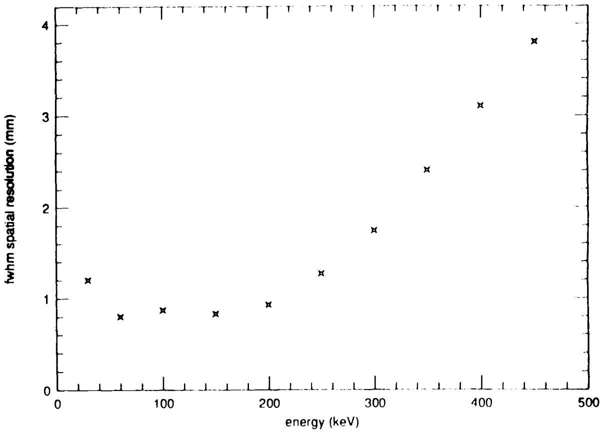

Through careful optimization of the imaging performance, millimeter spatial resolution can be achieved over a relatively large energy range with these imaging alkali halide scintillation detectors. If the goal is to optimize the detector performance for monochromatic γ-rays, spatial resolution better than 2.5 millimeters can be realized for energies up to 300 keV with reasonable quantum efficiency. Figure 4 shows a plot of fwhm spatial resolution versus energy for a detector optimized to detect γ-rays of a given energy. The crystal thickness is chosen so as to have at least 35% quantum efficiency at the energy of interest. The expected resolution for that crystal thickness is extrapolated using results from the Monte Carlo code, which itself has be normalized to fit the measured experimental points. As mentioned previously, our predictions do not take into account Compton scattering, which will be important at energies greater than ~ 200 keV. Thus the actual resolution may be slightly worse than indicated by the plot.

The overall shape of the plot can be understood as follows: At higher energies, the resolution is degraded due to the thickness of crystal required to yield reasonable quantum efficiency (above the K-edge of Iodine the required thickness scales like $(\text{energy})^3$). This effect is offset by the fact that for higher energy γ-rays more scintillation light is produced in the crystal (the resolution scales like $(\text{energy})^{-1/2}$ for crystal of fixed thickness). The resolution is relatively flat over the range 50 - 200 keV because it is dominated by the intrinsic resolution of the Hamamatsu phototube and by the thickness of the glass faceplate. Below ~ 50 keV the resolution begins to degrade due to the decrease in the amount of scintillation light produced by the low-energy γ-rays. There is a wide band from 30 - 300 keV where good resolution can be achieved, making these devices important for a variety of applications.

5. ACKNOWLEDGEMENTS

The authors wish to thank Baruch Fuchs of the LLNL optics shop for assistance in preparing the scintillation crystals. This research was performed in part under the auspices of the U.S. Department of Energy by Lawrence Livermore National Laboratory under contract number W-7405-ENG-48, and was partially supported by a grant from the NASA Gamma-Ray Astrophysics and Analysis Program. FAH is supported by a NASA Graduate Student Research Fellowship.

6. REFERENCES

1. Seiffert, M.D., Lubin, P.L., Hailey, C.J., Ziock, K.P., Harrison, F.A., Kahn, S.M., 'The Gamma-Ray Arcminute Telescope Imaging System: mechanical design and expected performance', *EUV, X-RAY, and Gamma-Ray Instrumentation for Astronomy and Atomic Physics* , Charles J. Hailey, Oswald H.W. Siegmund, Editors, Proc. SPIE 1159, 344-353 (1989).

2. Harrison, F.A., Kahn, S.M., Hailey, C.J., Ziock, K.P., Lubin, P.L., Seiffert, M.D., 'The Gamma-Ray Arcminute Telescope Imaging System: detector performance and imaging', *EUV, X-RAY, and Gamma-Ray Instrumentation for Astronomy and Atomic Physics* , Charles J. Hailey, Oswald H.W. Siegmund, Editors, Proc. SPIE 1159, 36-44 (1989).

3. Harrison, *et al.*, 1989.